Enhanced Immunosuppressive Capability of Mesenchymal Stem Cell-derived Small Extracellular Vesicles with High Expression of CD73 in Experimental Autoimmune Uveitis

Yanan Duan (m13994130098@163.com)
Tianjin Medical University Eye Hospital https://orcid.org/0009-0005-7804-7954

Xiteng Chen
Tianjin Medical University Eye Hospital

Hui Shao
University of Louisville

Yongtao Li
Tianjin Medical University Eye Hospital

Zhihui Zhang
Tianjin Medical University Eye Hospital

Huan Li
Tianjin Medical University Eye Hospital

Chuan Zhao
Tianjin Medical University Eye Hospital

Hong Xiao
Tianjin Medical University Eye Hospital

Jiawei Wang
Tianjin Medical University Eye Hospital

Xiaomin Zhang
Tianjin Medical University Eye Hospital https://orcid.org/0000-0003-4898-4152

Research Article

Keywords: mesenchymal stem cell, small extracellular vesicle, CD73, adenosine, autoimmune uveitis

Posted Date: January 30th, 2024

DOI: https://doi.org/10.21203/rs.3.rs-3866385/v1

Enhanced Immunosuppressive Capability of Mesenchymal Stem Cell-derived Small Extracellular Vesicles with High Expression of CD73 in Experimental Autoimmune Uveitis

Yanan Duan[1†], Xiteng Chen[1†], Hui Shao[2], Yongtao Li[1], Zhihui Zhang[1], Huan Li[1], Chuan Zhao[1], Hong Xiao[1], Jiawei Wang[1], Xiaomin Zhang[1*]

[†] Yanan Duan and Xiteng Chen have contributed equally to this study

[1] Tianjin Key Laboratory of Retinal Functions and Diseases, Tianjin Branch of National Clinical Research Center for Ocular Disease, Eye Institute and School of Optometry, Tianjin Medical University Eye Hospital, Tianjin, China

[2] Department of Ophthalmology and Visual Sciences, Kentucky Lions Eye Center, University of Louisville, School of Medicine, Louisville, KY, USA.

* Correspondence: Xiaomin Zhang (xzhang08@tmu.edu.cn);

Abstract

Background: Autoimmune uveitis is an inflammatory disease triggered by an aberrant immune response. Mesenchymal stem cell-derived small extracellular vesicles (MSC-sEVs) are emerging as potential therapeutic agents for this condition. CD73, an ectoenzyme present on MSC-sEVs, is involved in mitigating inflammation by converting extracellular adenosine monophosphate into adenosine. We hypothesize that the inhibitory effect of MSC-sEVs on experimental autoimmune uveitis (EAU) could be partially attributed to the surface expression of CD73.

Methods: To investigate novel therapeutic approaches for autoimmune uveitis, we

performed lentiviral transduction to overexpress CD73 on the surface of MSC-sEVs, yielding CD73-enriched MSC-sEVs (sEVs-CD73). Mice with IRBP-induced EAU were grouped randomly and treated with 50 μg MSC-sEVs, vector infected MSC-sEVs, sEVs-CD73 or PBS via single tail vein injection. We evaluated the clinical and histological features of the induced mice and analyzed the proportion and functional capabilities of T helper cells. Furthermore, T-cells were co-cultured with various MSC-sEVs *in vitro*, and we quantified the resulting inflammatory response to assess the potential therapeutic benefits of sEVs-CD73.

Results: Compared to MSC-sEVs, sEVs-CD73 significantly alleviates EAU, leading to reduced inflammation and diminished tissue damage. Treatment with sEVs-CD73 results in a decreased proportion of Th1 cells in the spleen, draining lymph nodes, and eyes, accompanied by an increased proportion of Treg cells. *In vitro* assays further reveal that sEVs-CD73 inhibit T-cell proliferation, suppress Th1 cells differentiation, and enhance Treg cells proportion.

Conclusion: Over-expression of CD73 on MSC-sEVs enhanced their immunosuppressive effects in EAU, indicating that sEVs-CD73 have the potential as an efficient immunotherapeutic agent for autoimmune uveitis.

Keywords: mesenchymal stem cell, small extracellular vesicle, CD73, adenosine, autoimmune uveitis

Background

Autoimmune uveitis is a complex and heterogenous inflammation that manifests with diverse symptoms, including blurred vision, photophobia and pain [1, 2]. Several therapeutic modalities, such as glucocorticoids (GCs) and immunosuppressive agents, are employed to address the intricacies of this condition. Predominantly, GCs stand as the primary choice in clinical uveitis treatment. However, their protracted usage is encumbered by drawbacks, which encompass adverse effects like cataracts, glaucoma, and systemic repercussions [3-5]. Other methodologies also exhibit certain limitations. Consequently, ongoing researches into novel therapies aspire to not only heighten treatment efficacy but also mitigate adverse effects, ultimately refining the comprehensive management of uveitis.

In recent years, some studies have assessed both the efficacy and safety of mesenchymal stem cells (MSCs) in addressing experimental autoimmune uveitis (EAU) in animal models [6-8]. MSCs, widely recognized for their regenerative and immunomodulatory functions, have been employed to attenuate diverse immune responses, including autoimmune disorders [9]. Nonetheless, the utilization of MSCs-based therapy not only presents challenges in cell product preservation and transport, but also elevates the risks associated with vessel obstruction, malignant transformation, and allogenic immunological rejection [10-13]. To mitigate these obstacles, attention has turned to their secretions, small extracellular vesicles (sEVs). These nano-sized vesicles play a pivotal role in shuttling nutrient substances to mediate recipient cell functions, mirroring the impact of their parent cells [14-16]. The lipid bilayer membrane structure

of sEVs could protect their cargo from degradation. Consequently, they have been extensively harnessed as ideal drug carriers and strategically modified for therapeutic interventions in various immune disorders. Furthermore, the utilization of MSC-derived sEVs (MSC-sEVs) holds promise for therapeutic agent applications, as they offer improved safety and stability compared to their parent MSCs. Nevertheless, the current immunosuppressive potency of MSC-sEVs falls short for clinical implementation, and ongoing research endeavors are dedicated to optimizing the use of MSC-sEVs by exploring their immunomodulatory mechanism [16].

CD73 is one of the key markers of MSCs. We previously proved that MSCs could exert their immunomodulatory capacity through the CD73 pathway in intraocular immune responses [17]. The ectoenzyme CD73, characterized as a glycosylphosphatidylinositol-anchored glycoprotein, plays a pivotal role in purinergic signaling [18]. It facilitates the conversion of extracellular pro-inflammatory adenosine triphosphate (ATP) into the anti-inflammatory adenosine (Ado) [19]. As the activity of CD73 is irreversible, ongoing research on CD73 holds promise, particularly in its potential to modulate immune responses via Ado production. Research has shown that human MSC-sEVs share similar surface markers with their parent cells, including CD73 [20]. Based on this premise, in this study, we investigated the immunosuppressive effect of CD73-overexpressed MSC-sEVs (sEVs-CD73) using EAU models, and found that compared to normal MSC-sEVs, sEVs-CD73 demonstrated stronger therapeutic effect in EAU.

Materials and methods

Animals

All female C57BL/6 mice (7–8 weeks old) purchased from GemPharmatech Co., Ltd. (China) were housed under specific pathogen-free (SPF) conditions. Animal care and experimentation were conformed to the Association for Research in Vision and Ophthalmology (ARVO) Statement. All animal procedures were approved by the Animal Care and Use Committee of Tianjin Medical University Eye Hospital (TMUEC).

Culture and Identification of Mesenchymal Stem Cells

Human umbilical cord MSCs were provided by Beijing Beilai Biological Co., Ltd. (China), and MSC isolation and culture were performed as previously described [21]. Various methods are available for the identification of MSCs, including flow cytometry and differentiation assays. According to International Society for Cell & Gene Therapy (ISCT), MSCs were identified by their capacity to express specific cell surface markers (CD73, CD90), and lack expression of hematopoietic lineage markers (CD34, CD45) [22]. Additionally, their ability to differentiate into adipocytes, chondrocytes, and osteocytes under defined conditions was demonstrated by staining *in vitro* and the expression of the target genes in MSCs was detected by Quantitative Real-time PCR (qRT-PCR).

Production and Transduction of Lentiviruses

Lentiviral vectors overexpressing CD73 and empty plasmids (pCDH-CMV-MCS-EF1-copGFP) (Hanbio Biotechnology, Shanghai, China) were packaged into human

embryonic kidney 293 T cells (HEK-293 T) following the manufacturer's instructions. The packaging plasmids and envelope plasmids were also involved in the transfection process. At 48 and 72h post-transfection, the lentiviral particles were harvested from the culture and subsequently concentrated by ultracentrifugation at 72000×g for 2 h. Subsequently, the viral titer was assessed using the serial dilution method, as outlined in previous studies [23].

Transfection and Supernatant Collection

Upon reaching approximately 60% confluency at passage 2, MSCs were exposed to a viral particle mixture with a multiplicity of infection (MOI) of 50 and 8 μg/ml polybrene (Sigma-Aldrich, St. Louis, USA) in the culture medium. Subsequently, we obtained normal MSCs (MSC-N), vector-infected MSCs (MSC-V), and CD73-overexpressed MSCs (MSC-CD73). The conditioned medium from the third to fifth passage was collected for the production of MSC-sEVs. MSCs were cultured with complete DMEM/F-12 (Gibco, California, USA) media containing 10% sEVs-free FBS (Gibco) and 100 U/mL penicillin and streptomycin (Gibco). To generate sEVs-free FBS, excess sEVs from FBS were removed by overnight centrifugation at 110,000×g, 4° C.

Quantitative Real-time PCR (qRT-PCR)

The qRT-PCR was conducted to assess mRNA expression levels of different MSCs (MSC-N, MSC-V, MSC-CD73). Total RNA extraction was performed using the TRIzol reagent (Invitrogen) following the manufacturer's instructions. Subsequently, cDNA was synthesized utilizing the RevertAid First Strand cDNA Synthesis Kit (Thermo Fisher, Massachusetts, USA). Each PCR reaction was set up in 384-well plates,

comprising FastStart SYBR Green Master (Roche, Basel, Switzerland), cDNA, and 0.25 uM forward and reverse primers. The relative mRNA expression levels of the target genes were determined using the $2-\Delta\Delta Cq$ method, with GAPDH serving as an internal standard [24]. The primer sequences used were as follows: CD73 forward: CCAGTACCAGGGCACTATCTG, reverse: TGGCTCGATCAGTCCTTCCA; GAPDH forward: AGGTCGGTGTGAACGGATTTG, reverse: GGGGTCGTTGATGGCAACA.

Collection of Mesenchymal Stem Cell-derived Small Extracellular Vesicles

The supernatant of both uninfected and infected MSCs was collected after 48 h of incubation and separated by ultracentrifugation in order to obtain each group of MSC-sEVs. After centrifugation at 200×g for 10 minutes at 4℃, 2000×g for 20 minutes at 4℃, and 10,000×g for 30 minutes at 4℃, the resulting supernatant was further centrifuged twice at 110,000g for 70min at 4℃ to obtain a high concentration of MSC-sEVs [25]. All ultracentrifugation steps were performed on an Optima XLA/I centrifuge equipped with an An-45Ti rotor (Beckman-Coulter, California, USA). The final pellets were resuspended in sterile PBS (Gibco), and the concentration was measured using a BCA protein assay kit (Solarbio, China).

Identification of Mesenchymal Stem Cell-derived Small Extracellular Vesicles

To accurately characterize and distinguish different types of MSC-sEVs, various techniques were utilized in this study. Samples were quickly fixed with paraformaldehyde (Sigma-Aldrich) for 5 minutes and applied to carbon copper grids. Negative staining was performed using 2% uranyl acetate solution (Sigma-Aldrich).

After drying, direct visualization of the MSC-sEVs was conducted using Transmission Electron Microscopy. Additionally, nanoparticle tracking analysis (NTA) was utilized to measure the size and concentration of MSC-sEVs in a liquid medium. The particle size was analyzed using NTA software (version 3.3, Nanosight). For identification of various protein markers associated with different MSC-sEVs, Western blot was used. The isolated MSC-sEVs were lysed to release their protein content, which was then separated by polyacrylamide gel electrophoresis (SDS-PAGE) based on size and charge. The separated proteins were transferred onto a polyvinylidene difluoride (PVDF) membrane (Sigma-Aldrich) and incubated with a 5% non-fat dried milk to prevent non-specific binding of the antibody. The membrane was then probed with antibodies specific to MSC-sEVs-associated proteins, including CD9 (Abcam, UK), CD63 (Abcam), TSG-101 (Abcam), CD73 (Abcam) and β-actin (Abcam). Additionally, the expression of CD73 on the surface of MSC-sEVs was also identified using ELISA kits, following the manufacturer's instructions (R&D Systems).

Induction and Treatment of Experimental Autoimmune Uveitis

EAU in C57BL/6 mice was induced by immunization with an emulsion comprising equal volumes of complete Freund's adjuvant (CFA, Sigma Aldrich) and 5 mg/mL desiccated Mycobacterium tuberculosis (TB, Sigma-Aldrich), as well as 300 μg IRBP651-670 (LAQGAYRTAVDLESLASQLT, Shanghai Hanhong Chemical Co., Ltd., Shanghai, China) in PBS. This emulsion was then applied to four spots on the tail base and flank. In addition, mice were intraperitoneally administered 500 ng pertussis toxin (PTX, List Biological Laboratories, California, USA) on the day of immunization and

24 h post-immunization. Immunized mice were randomly placed into cages assigned to different groups, including PBS, MSC-sEVs (sEVs-N), vector-infected MSC-sEVs (sEVs-V), and sEVs-73 group. On day 11 post immunization, different groups of mice were injected via tail vein with 50 μg diverse MSC-sEVs respectively or equal volume of PBS.

Clinical and Histological Assessment of Experimental Autoimmune Uveitis

EAU mice were examined every other day by head-mounted indirect fundoscopy from day 9 to day 21 post-immunization. On the 17th day post-immunization, mice were euthanized, and their eye tissues were fixed in 4% paraformaldehyde, paraffin-embedded, sectioned (4μm), and stained with hematoxylin and eosin (H&E). The histopathological changes of retina were examined and scored. The incidence and severity of inflammation were assessed according to the criteria of Caspi [26].

Optical Coherence Tomography

On the 17th day post-immunization, a total of six mice per group were anesthetized, and the pupils were dilated with 0.1% tropicamide. The mice were then placed in a prone position, and a corneal contact lens was used to stabilize the eye. Spectralis optical coherence tomography (OCT) (Heidelberg, Germany) was used to scan the retina, and the images were scored based on the criteria previously established by Gadjanski and colleagues [27].

Flow Cytometry Detection of Inflammatory Cells

Mice were sacrificed on day 17 after immunization and their eyeballs, spleens (SP) and lymph nodes (LN) were separated and ground. To prepare single lymphocyte

suspension, the spleen was lysed with red blood cell lysis buffer (Sigma), while the eyeball tissue was digested with 1mg/ml of collagenase D (Sigma-Aldrich) for 1 hour. The resulting cell suspensions were filtered through a 70-μm filter and then centrifuged. Part of these cells were incubated in a 96-well plate with 50 ng/mL phorbol 12-myristate 13-acetate (Sigma), 1 μg/mL ionomycin (Sigma), and 1 μg/mL brefeldin A (Abcam, Cambridge, USA). After incubation of 4.5 hours, these cells were utilized to assess the ratio of Th1 and Th17 cells, while the remaining cells were prepared into single cell suspensions to determine the proportion of Treg cells.

The cells were stained with fluorescein-conjugated anti-mouse CD4 antibody for 30 min at 4°C. Further fixation and permeabilization were performed according to the manufacturer's instructions. After staining with corresponding antibodies, the proportion of IFN-γ, IL-17A, and FOXP-3 was detected by FACSCalibur flow cytometer (BD Biosciences, USA) and analyzed using flow cytometry software (FlowJo, USA). All antibodies were obtained from BioLegend.

Assay of T-cell Proliferation *in vitro* by Carboxyfluorescein Diacetate Succinimidyl Ester (CFSE)

The 96-well plates were precoated with 10 μg/mL anti-mouse CD3 mAb (BioLegend) and 5 μg/mL anti-mouse CD28 mAb (BioLegend) to stimulate $CD4^+$T-cells. The total $CD4^+$T-cells were isolated from spleens of naive mice by positive $CD4^+$T-cell isolation kit (Miltenyi Biotec, California, USA). The cells were then labeled with 1 μM carboxyfluorescein diacetate succinimidyl ester (CFSE) (Invitrogen) for 10 min and co-cultured with MSC-sEVs at a concentration of 10 μg/ml. After 72 hours of incubation,

the CFSE fluorescence intensity was measured by FACS and analyzed by FlowJo.

T-cell Differentiation Assays *in vitro*

Naive $CD4^+$T-cells from spleens of naive mice were isolated using a positive isolation kit (Miltenyi Biotec). These purified cells were seeded at a density of $2x10^5$ cells/well in 96-well plates pre-coated with anti-CD3/CD28 and then cultured under Th1, Th17, and Treg differentiation conditions, respectively. After cultivation, the corresponding antibody was stained. Th1, Th17 and Treg cell populations were analyzed by flow cytometry.

For Th1 polarization, cells were cultured in RPMI-1640 cell culture medium (Gibco) (supplemented with IL-12 at 20 ng/mL and anti-IL-4 at 10 μg/mL). For Th17 polarization, cells were cultured in RPMI-1640 cell culture medium (supplemented with IL-6 at 20 ng/mL, anti-IL-4 at 10 μg/mL, anti-IFN-γ at 10 μg/mL, and TGF-β1 at 2ng/mL). For Treg polarization, cells were cultured in RPMI-1640 cell culture medium (supplemented with TGF-β1 at 5 ng/mL and IL-2 at 20 ng/mL). After 5 days of culture, the cells were collected and analyzed using FACS. Recombinant cytokines were purchased from R&D Systems (Minneapolis, USA), while antibodies against these cytokines were purchased from BD Biosciences (California, USA).

Quantification of Adenosine Levels using high performance liquid chromatography (HPLC)

Naive T-cells were cultured in RPMI-1640 cell culture medium supplemented with anti-CD3 and anti-CD28. After three days of culture, 50 μL cell supernatant was collected and transferred to a 1.5 ml EP tube. Subsequently, 50 μL of methanol was added,

followed by thorough vortex mixing. Then, 100 μL of acetonitrile was added, vortexed for 30 seconds, and centrifuged at 12,000 rpm for 10 minutes at 4℃. The supernatant was collected for mass spectrometry detection. The subsequent performance liquid chromatography (HPLC) procedures were conducted using the ACQUITY UPLC I-Class/Xevo TQ-XS (Waters, Massachusetts, USA). A series of Ado standards ranging from 200 pg/ml to 20,000 pg/ml was prepared and stored at 4℃. A standard curve was constructed using the average peak area as the x-axis and Ado concentration as the y-axis, with the regression equation calculated. The chromatographic column used was Waters BEH C18 (2.1*100 mm, 1.7 μm), maintained at 30℃.

Statistical Analysis

The data obtained from all experiments are expressed as mean±standard deviation (SD). In contrast, the one-way analysis of variance (one-way ANOVA) was utilized determine the statistical significance. These data were analyzed using the software GraphPad Prism 9.4 (GraphPad Software, USA). The criterion for statistical significance was set at $P < 0.05$.

RESULTS

Transfection of lentivirus into mesenchymal stem cells

To obtain a high expression lentivirus vector of CD73, we packaged the constructed plasmid into HEK-293T cells and measured the titer of the resulting supernatant after concentration. We found that the transfected HEK-293 T cells exhibited high green fluorescent protein (GFP) fluorescence expression under a fluorescence microscope. The titer of the CD73-overexpressed lentivirus reached $7x10^7$ TU/ml, while that of the control vector was $2x10^9$ TU/ml (Figure 1A, B). The MSCs were then transduced with the virus, and high fluorescence expression was observed under a fluorescence microscope 48 hours post-transfection (Figure 1C).

Identification of mesenchymal stem cells

The microscopic examination revealed the spindle-shaped morphology of MSCs adhering to the culture flask walls. Furthermore, under specific differentiation conditions, MSCs demonstrated their ability to differentiate into osteocytes, chondrocytes, and adipocytes (Supplementary figure S1). Additionally, the flow cytometry identification of surface markers on MSCs can be referenced based on our previous findings [28].

Identification of mesenchymal stem cell-derived small extracellular vesicles

Using Nanosight and TEM techniques, we analyzed the size and morphology of sEVs purified from the conditioned medium of MSCs. Nanosight analysis revealed an average diameter of approximately 100nm for MSC-sEVs (Figure 2A). TEM images illustrated that sEVs-N, sEVs-V, and sEVs-CD73 were uniformly sized, circular and

had double-layered membrane vesicular structures, consistent with the typical features of sEVs (Figure 2B). Western blotting results confirmed the expression of CD9, CD81, TSG101, and CD73 in all groups, with successful high expression of CD73 in the sEVs-CD73 group (Figure 2C). Real-time PCR analysis showed high expression of the target gene post-viral infection in MSCs, corroborated by fluorescence microscopy 48 hours post-transfection (Figure 2D). ELISA results indicated higher levels of the target protein in sEVs-CD73 compared to the other groups (Figure 2E).

Augmented suppression of experimental autoimmune uveitis through over-expression of CD73 on mesenchymal stem cell-derived small extracellular vesicles by inhibiting inflammatory cell infiltration

To evaluate the therapeutic efficacy of sEVs-CD73, we administered tail vein injections to mice on the 11th day post-immunization. Clinical scoring indicated that inflammatory changes in the fundus occurred around the 11th day and peaked at approximately 17 days post-immunization (Figure 3A). We observed that injection of sEVs-N and sEVs-V effectively halted the progression of EAU, and this immunomodulatory effect was further strengthened upon over-expression of CD73. Fundus images showed severe inflammation and partial linear lesions at the peak of the disease in the PBS-treated group. The sEVs-N and sEVs-V group displayed less pronounced inflammatory responses. Notably, treatment with sEVs-CD73 demonstrated the most significant inhibition of these alterations among the four groups (Figure 3B). Histological results analysis confirmed these findings, with the sEVs-CD73-treated mice exhibiting fewer infiltrating inflammatory cells, reduced retinal

folds, detachment, and granulomas (Figure 4).

T-cells, including Th1, Th17 and Treg cells, play crucial roles in cell-mediated immunity. At the peak of the disease, we collected tissues such as eyeballs, spleen, and draining lymph nodes from mice to detect the proportion of different T-cell subsets in each group. Flow cytometric results showed an increase in the proportions of Th1 cells in the sEVs-CD73 group compared to the sEVs-N and sEVs-V groups, suggesting sEVs-CD73 have an enhanced inhibitory effect on Th1 cells. However, unexpectedly, CD73 over-expression did not significantly alter the inhibitory effect of MSC-sEVs on Th17 cells (Figure 5A). Moreover, the proportion of Treg cells also exhibited significant changes in the spleen and draining lymph nodes. As illustrated in Figure 5B, the proportion of Treg cells in the sEVs-CD73 group was significantly higher than that in the sEVs-N and sEVs-V groups. These results indicate that MSC-sEVs with high CD73 expression enhance their stimulative effects on Treg cells.

Amplified inhibitory efficacy of mesenchymal stem cell-derived small extracellular vesicles on T cell proliferation in co-culture via CD73 over-expression

To assess the effect of MSC-sEVs from different groups on T-cell proliferation, we isolated $CD4^+$ T-cells from the spleen and draining lymph nodes of untreated mice using a magnetic bead positive selection kit. These T-cells were co-cultured with a certain concentration of MSC-sEVs from each group, and CFSE expression was observed after four days of culture. Flow cytometric results revealed that sEVs-CD73 exhibited a more pronounced inhibitory effect on T-cell proliferation compared to sEVs-N and sEVs-V groups at a concentration of 10 μg/ml (Figure 6A-B).

Enhanced inhibition of Th1 cell differentiation and promotion of Treg cell differentiation in co-culture via CD73 over-expression on mesenchymal stem cell-derived small extracellular vesicles

Naive T-cells combined with 10 μg/ml of various MSC-sEVs in specific differentiation conditions were cultured for 4 days to assess immune cell proportions. Flow cytometric analysis revealed that MSC-sEVs with CD73 over-expression exhibited a significantly heightened inhibitory effect on Th1 cells and a pronounced promotional effect on Treg cells, in contrast to sEVs-N and sEVs-V. Notably, their impact on Th17 cells remained unchanged (Figure 6C-H).

CD73-enriched mesenchymal stem cell-derived small extracellular vesicles increased adenosine levels in the T-cell supernatant

Using HPLC, the Ado content in the supernatant of Naive T-cells co-cultured with different groups of MSC-sEVs was analyzed. The linear regression equation for the Ado standard curve was Y=13.8533X+3980.22, with an R2 value of 0.9991 (Figure 7A). A distinct peak at 1.62 min was observed (Figure 7B). The addition of sEVs-N and sEVs-V led to an increase in Ado production compared to the control group, although not reaching statistical significance. However, the sEVs-CD73 group showed a significant increase in adenosine compared to the other three groups (Figure 7C).

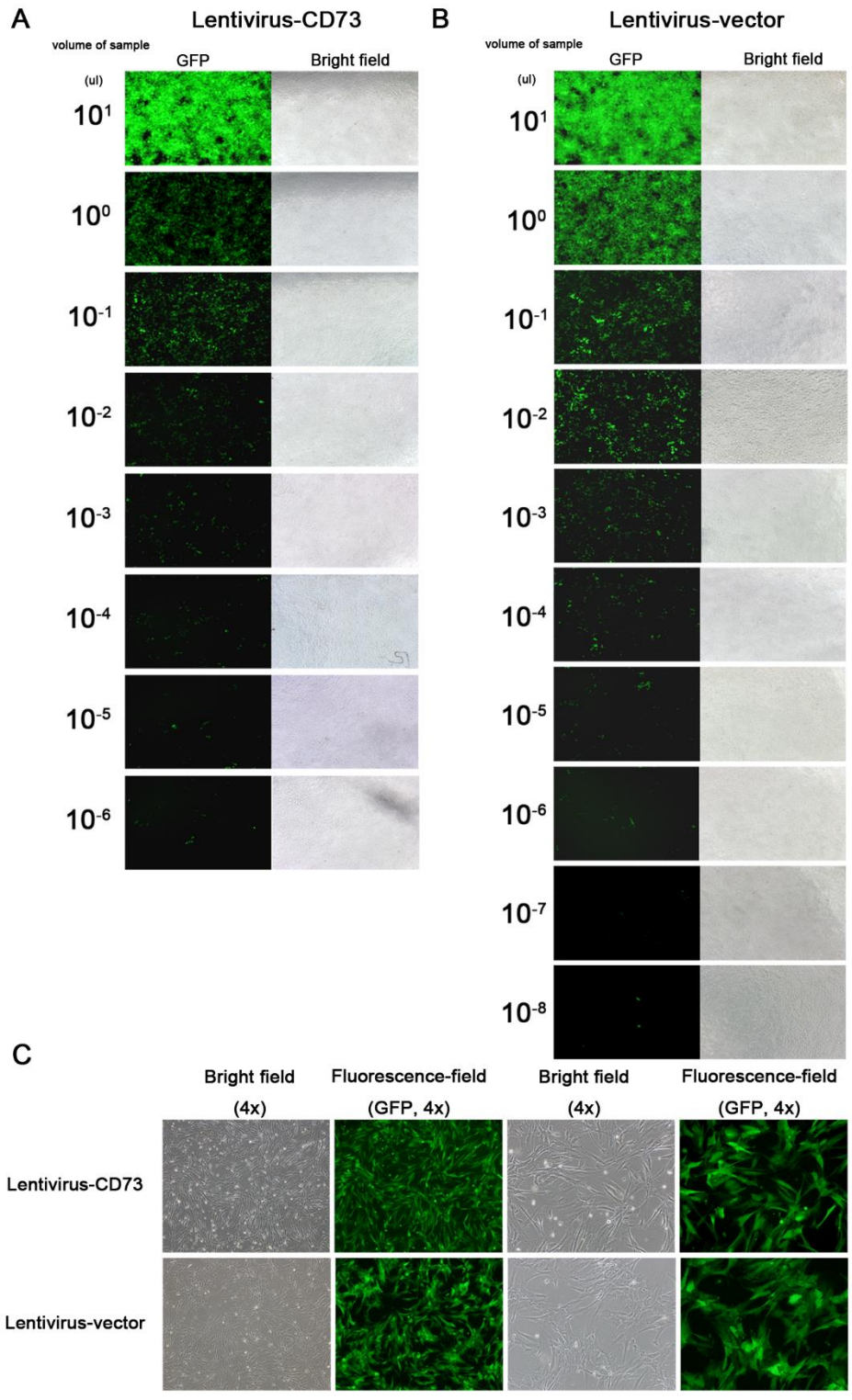

Figure 1. Lentiviral titration assays and transduction. (A-B) Lentivirus titration assays depict the over-expression of CD73 and empty vector controls, with viral titers reaching approximately $7x10^7$TU/ml and $2x10^9$TU/ml, respectively. (C) Bright/dark field images reveal targeted gene expression 48 hours post-lentiviral infection of MSCs.

The high expression of GFP confirms the successful transduction of the lentivirus.

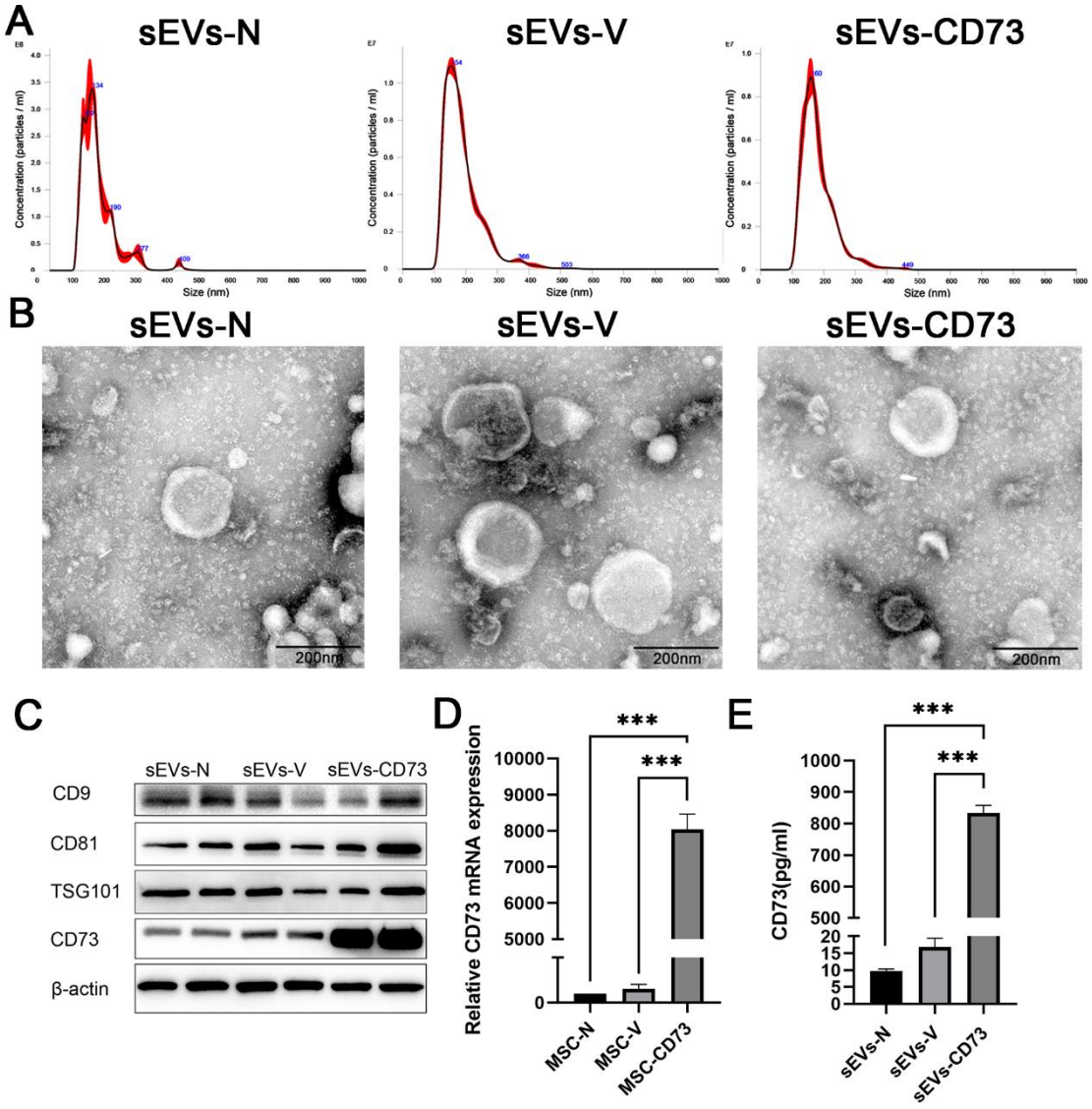

Figure 2. Identification of MSC-sEVs. (A) Nanosight analysis depicting the size distribution of various MSC-sEVs. (B) TEM images illustrating the morphology of various MSC-sEVs. Scale bar=200 nm. (C) Western blotting results indicating the expression of CD9, CD81, TSG101, and CD73 in sEVs-N, sEVs-V, and sEVs-CD73 group. To maintain conciseness, cropping was performed. Full-length blots were presented in Supplementary Figure S2. (D) Real-time PCR results showing robust expression of the target gene after viral infection of MSCs. (E) ELISA results

demonstrating elevated levels of the target protein in sEVs-CD73 compared to the other groups. Mean±SD, n=3 per group, one-way ANOVA test. ***: P < 0.001.

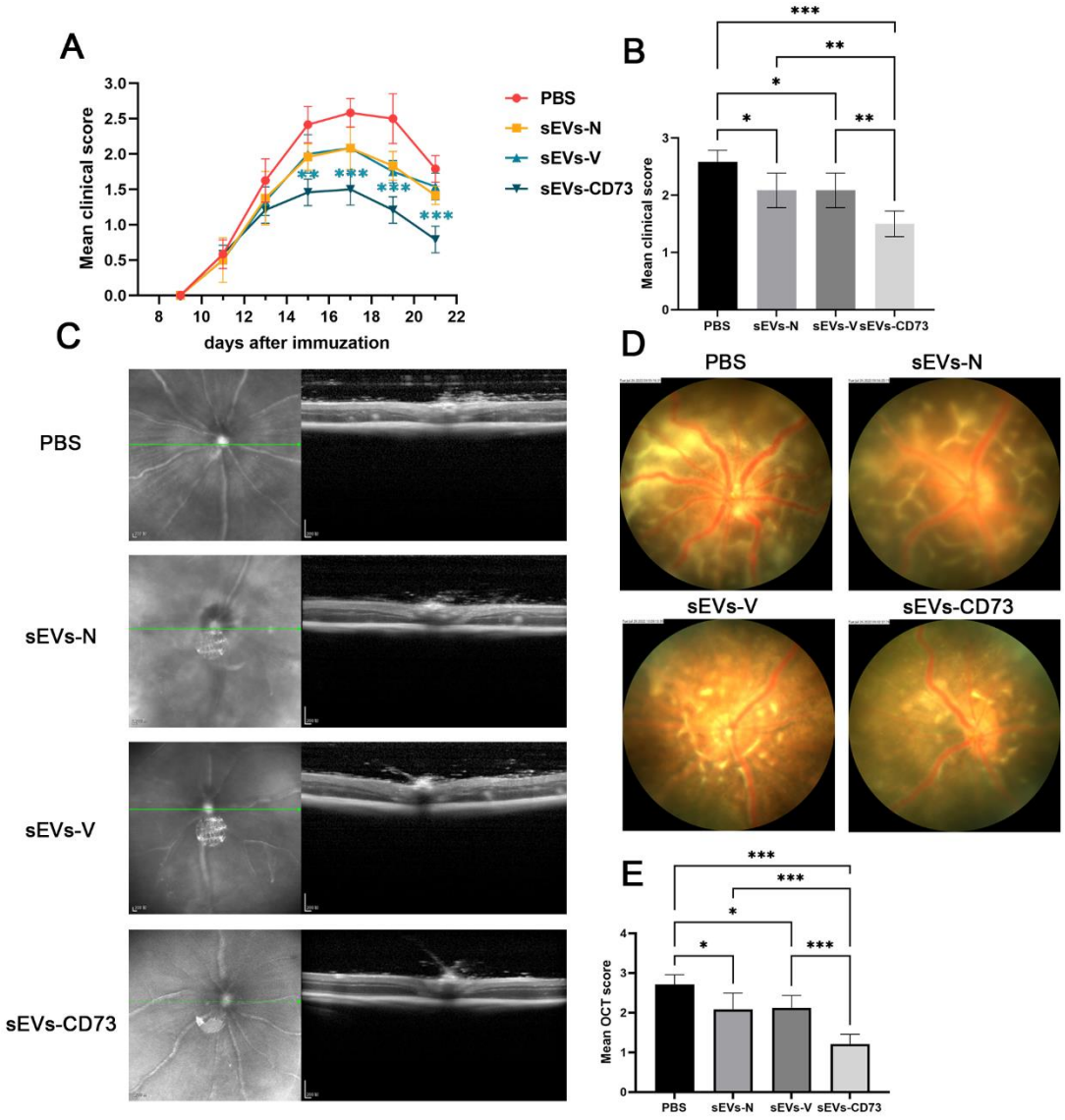

Figure 3. Over-expression of CD73 enhanced the therapeutic efficacy of MSC-sEVs in EAU. (A-B) Mean clinical scores of mice treated with tail vein injection of 50ug sEVs recorded every 2 d from day 9 to day 21 post-immunization. (C, E) On day 17 post-immunization, OCT was conducted, and the outcomes were quantified and presented as OCT scores. (D) The fundus imaging of each sEVs-treated group on day 17 post-immunization. Mean±SD, n=6 per group, one-way ANOVA test. *: P＜0.05;

**: P＜0.01; ***: P＜0.001.

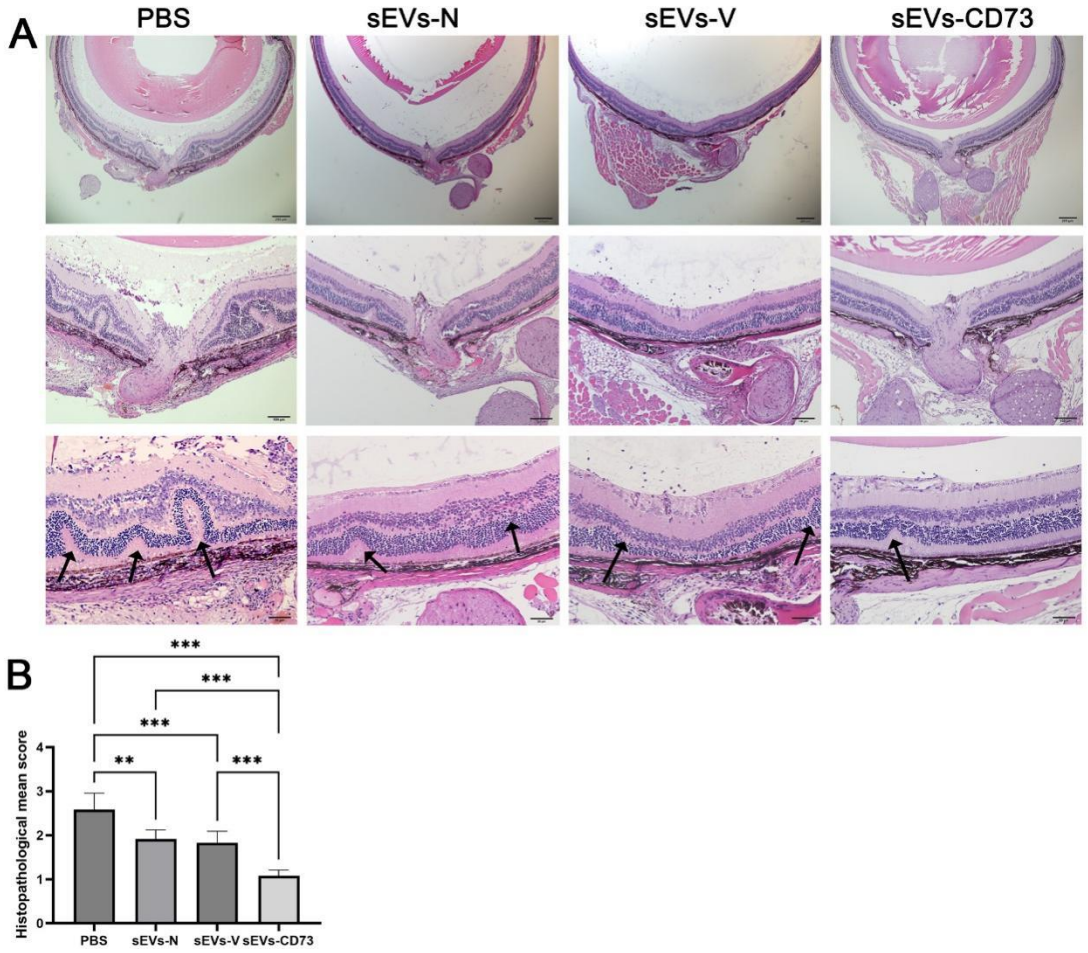

Figure 4. Treatment with sEVs-CD73 in EAU mice showed reduced inflammatory cell infiltration, retinal folds and granulomas. (A) Representative H&E-stained retinal cross-sections from different treatment groups. The black arrows indicate retinal folds and detachments near the optic disk. (B) Quantitative histopathological scores of the retina in each group. Mean±SD, n=6 per group, one-way ANOVA test. **: P＜0.01; ***: P<0.001.

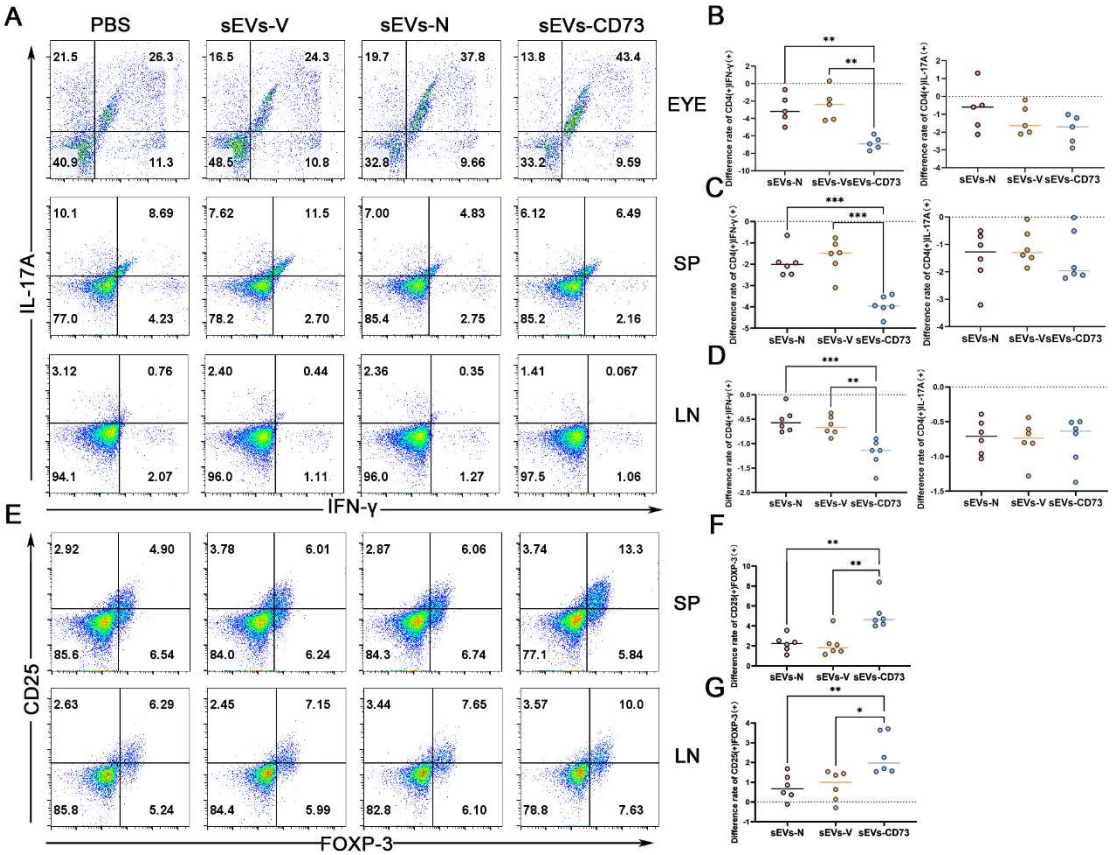

Figure 5. sEVs-CD73 treatment in EAU mice inhibited Th1 cells and increased Treg cells compared to sEVs-N. (A) Flow cytometric results of the proportions of Th1 ($CD4^+IFN\text{-}\gamma^+$) cells and Th17 ($CD4^+IL\text{-}17A^+$) cells in the eyeballs (n=5), draining lymph nodes (n=6) and spleen (n=6) of mice from different groups. (B) Flow cytometric results of the proportions of Treg ($CD4^+FOXP3^+CD25^+$) cells in the draining lymph nodes (n=6) and spleen (n=6) of mice from different groups. (C-G) The flow cytometric results of sEVs-N group, sEVs-V group, and sEVs-CD73 group were separately analyzed to calculate the difference compared to the blank control. Mean±SD, one-way ANOVA test. *: $P<0.05$; **: $P<0.01$; ***: $P<0.001$.

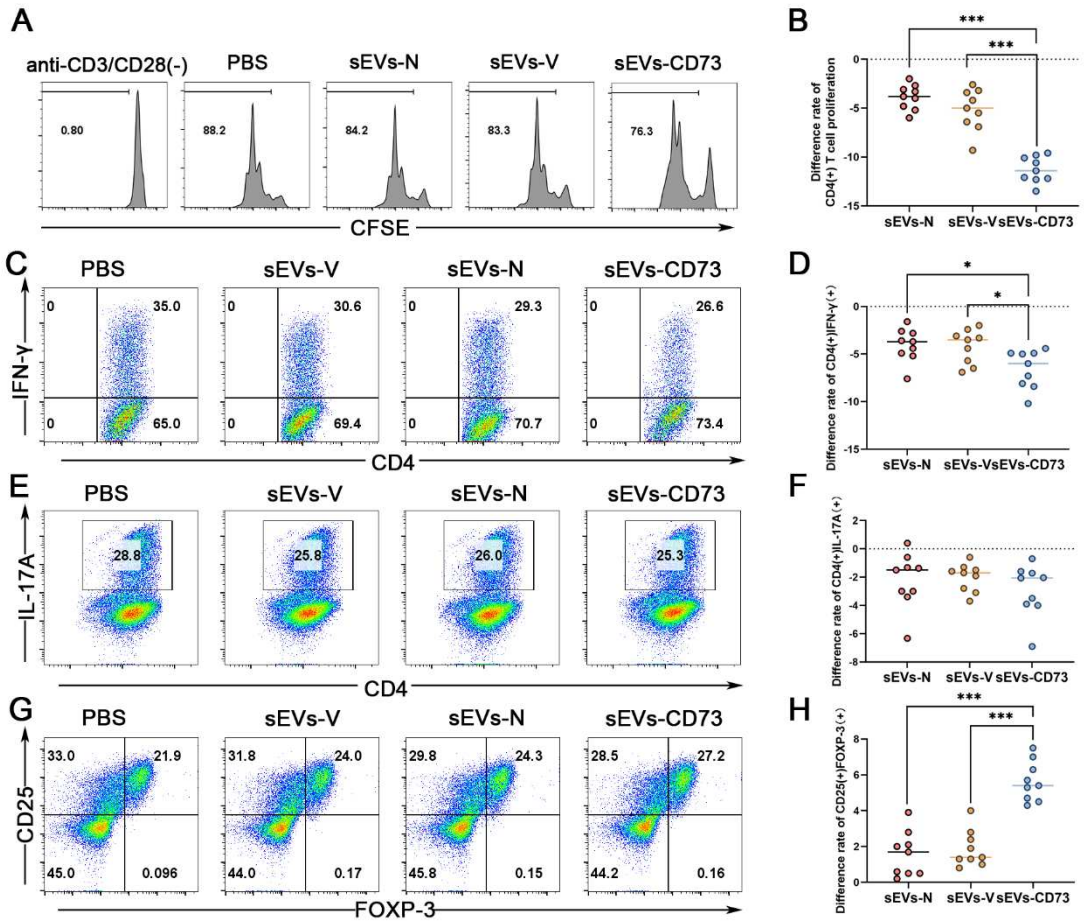

Figure 6. sEVs-CD73 stimulated T-cell proliferation and Th1 cell differentiation, while inhibiting Treg cells *in vitro*. (A, B) *In vitro* inhibition of T-cell proliferation by sEVs-CD73 compared to other groups. (C, D) *In vitro* inhibition of Th1 cell differentiation by sEVs-CD73 compared to other groups. (E, F) *In vitro* unchanged effect of Th17 cell differentiation by sEVs-CD73 compared to sEVs-N and sEVs-V groups. (G, H) *In vitro* promotion of Treg cell differentiation by sEVs-CD73 compared to other groups. Mean±SD, n=3 per group, one-way ANOVA test. All experiments were independently repeated 3 times. *: P＜0.05; **: P＜0.01; ***: P<0.001.

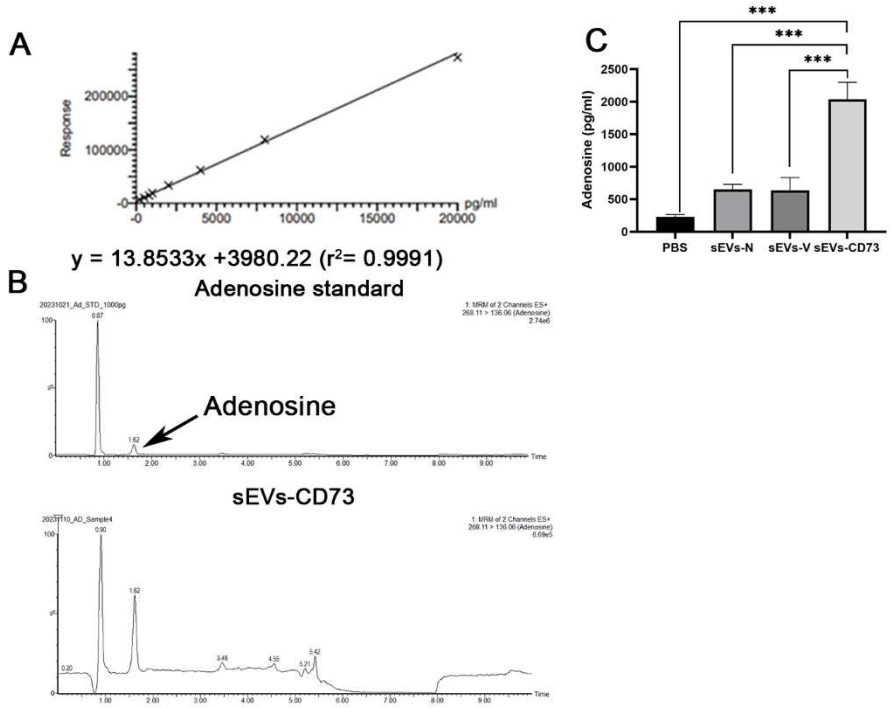

Figure 7. sEVs-CD73 facilitates the generation of adenosine *in vitro*. (A) The linear regression equation of Ado standard curve. (B) The chromatographic peak of Ado in sEVs-CD73 group detected by HPLC. (C) After co-culturing with T-cells, cell supernatant from the sEVs-CD73 group exhibited the highest proportion of secreted Ado among the four groups. Mean±SD, n=3 per group, one-way ANOVA test. ***: P ＜0.001.

Discussion

Our study established that, in comparison to the control group, MSC-sEVs exhibiting elevated CD73 expression exerted a more robust suppressive effect on the progression of EAU. *In vivo* experiments indicated that sEVs-CD73 can significantly reduce tissue infiltration of EAU in mice compared to normal MSC-sEVs. This alteration may be achieved by inhibiting T-cell proliferation, reducing the Th1 ratio,

and increasing the Treg ratio. *In vitro* results were consistent with those observed *in vivo*. Moreover, we speculated that the suppressive effect of sEVs-CD73 on EAU was likely mediated by the increased production of Ado.

MSCs and their secreted sEVs are considered to possess discernible immunosuppressive capabilities. MSC-sEVs, with their heightened stability, present distinct advantages in transportation and storage compared to MSCs. Therefore, MSC-sEVs have emerged as an attractive therapeutic tool for various immune-related diseases, including multiple sclerosis [29], inflammatory bowel disease [30-32], and autoimmune uveitis [21, 33]. However, our previous findings confirm the inherent inflammation-regulating capacity of MSC-sEVs falls short of producing robust inhibitory effects on EAU [21]. This limitation necessitates the utilization of a substantial quantity of MSC-sEVs for clinical translation, incurring both financial and resource expenditures. To enhance the anti-inflammatory properties of MSC-sEVs, scientists have directed their attention towards drugs with potent anti-inflammatory effects and loaded them onto MSC-sEVs via methods such as sonication, electroporation, chemical modification, extrusion and transfection [28, 34].

Under normal physiological conditions, cells release a minimal amount of ATP. However, in states of inflammation, damage, or toxicity, a substantial amount of ATP is extracellularly released, and its degradation rate is considerably lower than its production rate, exacerbating the occurrence of inflammation. ATP clearance predominantly relies on the CD39-CD73 pathway. In this process, ATP is initially degraded to ADP and AMP, ultimately degraded by CD73 to Ado [19]. Subsequently,

Ado acts on various immune cells, including mast cells, neutrophils, dendritic cells, macrophages, and lymphocytes, by binding to one or more Ado receptors on the cell surface (A1, A2A, A2B, and A3) [35]. Among them, the A2A receptor serves as the principal Ado receptor governing lymphocyte responses. The A2A knockout models suggest that activation of the A2A receptor inhibits the production of certain inflammatory factors, such as IFN-γ and IL-4 [36, 37], while concurrently reducing the secretion of IL-2 [36] by naive $CD4^+$ T-cells, thereby diminishing T-cell proliferation [38, 39]. Furthermore, A2A receptor activation can upregulate the expression of negative co-stimulatory molecules such as cytotoxic T-lymphocyte antigen 4 (CTLA-4) and programmed cell death protein 1 (PD-1), while downregulating the expression of positive co-stimulatory molecule CD-40L [38]. For Treg cells, the surface expression of CD39 and CD73 allows for the breakdown of ATP and ADP, leading to the generation of Ado [40]. The generated Ado not only directly influences T effector cells but can also reciprocally act on Treg cells by activating the A2A receptor, serving as an autocrine regulatory factor for Treg cells [41]. Thus, Ado and its A2A receptor play a role in suppressing inflammation in lymphocyte-mediated immune responses. Unfortunately, due to the short half-life of Ado, achieving prolonged inflammation suppression through direct elevation of Ado concentration is challenging. Therefore, drugs that interfere with Ado production and breakdown have become subjects of exploration.

As a rate-limiting enzyme in the degradation process of ATP, CD73 plays a crucial role in Ado production. CD73, also known as ecto-5'-nucleotidase (5'-NT, eN, eNT, NT5E), have broad potential in immunology, especially in autoimmune uveitis [42-

44]. As one of the surface markers of MSCs, CD73 is considered to be involved in the immune regulation process of MSCs. Research has suggested that the immunomodulatory effects of MSCs are predominantly mediated by Ado, and inhibiting CD73 expression and blocking A2A receptor signaling can both suppress the function of MSCs [45]. Chen et al. first reported that the surface CD73 of MSCs can catalyze the production of Ado, which, upon binding to the A2A adenosine receptor, inhibits the proliferation of Th1 cells [17]. Further research suggested that MSCs can generate a large amount of Ado through the CD73 pathway, and MSCs can indirectly suppress inflammation by upregulating the proportion of Tregs through the Ado pathways [46]. These findings suggest a potential mechanism through which MSCs could exert their immunomodulatory effects on EAU. As CD73 is also expressed on MSC-sEVs, targeting CD73 may also enhance the immunosuppressive potential of MSC-sEVs and reduce the amount of MSC-sEVs needed for clinical applications.

In recent years, many researchers have successfully overexpressed CD73 on the surface of cells [47, 48]. However, limited studies have focused on the over-expression of CD73 in MSC-sEVs. Our study successfully constructed sEVs-CD73 through lentiviral transduction. We speculated that sEVs-CD73 may promote Ado generation and regulate the Th1/Th17/Treg cell balance by interacting with $CD4^+$ T-cells via CD73, thereby creating an immune-suppressive microenvironment. To validate our hypothesis, mice immunized with IRBP651-670 were administered engineered MSC-sEVs via tail vein injection at the onset of the disease. The experimental results were generally consistent with our predictions. However, over-expression of CD73 seems to have no

impact on the proportion of Th17 cells. Currently, conflicting data exists for the role of CD73 in Th17 cells. The prevailing view suggests that CD73 has an inhibitory effect on the proportion of TH17 cells [49], and MSCs can regulate the proliferation of Th17 cells and the secretion of cytokines, such as IL-17A, through the Ado generation pathway mediated by CD39 [17, 50]. However, some scholars have proposed different viewpoints. They argue that the absence of CD73 does not affect the differentiation, recruitment, or function of Th17 cells in experimental autoimmune encephalomyelitis (EAE). They speculate that Th17 cells might indeed limit their activation by upregulating the CD39/CD73 enzyme complex, but the removal of ATP, rather than the generation of Ado, may play a more crucial role [51]. Our HPLC results revealed an increase in Ado content in the sEVs-CD73 group after *in vitro* cultivation, aligning with this speculation.

From our studies, engineering MSC-sEVs with enhanced CD73 expression emerges as a promising avenue for advancing sEVs-based therapies in the realm of autoimmune uveitis. This strategy ensures both biological safety and excellent immune regulation, allowing for the full utilization of MSC-sEVs as a natural immunosuppressive nanomaterial.

Conclusions

Overall, these findings indicated that both MSC-sEVs and sEVs-CD73 exhibited suppressive effects on EAU, with the latter showing significantly enhanced therapeutic efficacy. To facilitate clinical translation, future research should focus on the elucidating

the mechanism of sEVs-CD73 in EAU and on efficient production of sEVs-CD73.

Abbreviations

MSCs: mesenchymal stem cells; sEVs: small extracellular vesicles; MSC-sEVs: mesenchymal stem cell-derived small extracellular vesicles; EAU: experimental autoimmune uveitis; sEVs-CD73: CD73-overexpressed MSC-sEVs; GCs: glucocorticoids; ATP: adenosine triphosphate; Ado: adenosine; SPF: specific pathogen-free; ARVO: Association for Research in Vision and Ophthalmology; TMUEC: Tianjin Medical University Eye Hospital; ISCT: International Society for Cell & Gene Therapy; qRT-PCR: quantitative real-time PCR; HEK-293 T: human embryonic kidney 293 T cells; MOI: multiplicity of infection; sEVs-N: normal MSC-sEVs; sEVs-V: vector-infected MSC-sEVs; MSC-N: normal MSCs; MSC-V: vector-infected MSCs; MSC-CD73: CD73-overexpressed MSCs; NTA: nanoparticle tracking analysis; PVDF: polyvinylidene difluoride; CFA: complete Freund's adjuvant; TB: mycobacterium tuberculosis; PTX: pertussis toxin; H&E: hematoxylin and eosin; OCT: spectralis optical coherence tomography; SP: spleens; LN: lymph nodes; CFSE: carboxyfluorescein diacetate succinimidyl ester; HPLC: liquid chromatography; SD: standard deviation; ANOVA: analysis of variance; GFP: green fluorescent protein; CTLA-4: cytotoxic T-lymphocyte antigen 4; PD-1: programmed cell death protein 1; EAE: experimental autoimmune encephalomyelitis

Supplementary Information

Additional file 1: Figure S1.bmp. Identification of MSCs. Specific differentiation conditions promote successful differentiation of MSCs into osteoblasts, chondrocytes, and adipocytes.

Additional file 2: Figure S2.bmp. The Western blot gel image depicted protein expression patterns in sEVs-N, sEVs-V, sEVs-CD73. To minimize cross-contamination between different antibodies, two gels were prepared to detect the expression of surface proteins on distinct groups of sEVs. Gel 1 was utilized for detecting CD9, CD81 and TSG101, while Gel 2 was employed for incubating with CD73. Both gels were loaded with the same amounts of samples, and β-actin was probed on each gel to ensure consistency in loading. Lane assignments were as follows: Lane 1, 2 (sEVs-N); Lane 3, 4 (sEVs-V); Lane 5, 6 (sEVs-CD73). For conciseness, the images were cropped, as indicated by the boxed area.

Declarations

Ethics approval and consent to participate

The animal studies were approved by the Laboratory Animal Care and Use Committee of Tianjin Medical University Eye Hospital (TMUEC) (No. TJYY2019103022). The approved project was titled "The Mechanism Study of MSCs-exo Regulating Th17/Treg Cells in Treating Mouse EAU via CD39/CD73/Adenosine Pathway." The date of approval is October 30, 2019.

Consent for publication

Not applicable.

Availability of data and materials

The datasets used or analyzed during the current study are available from the corresponding author on reasonable request.

Competing interests

The authors have declared that no competing interest exists.

Funding

This research was funded by the National Natural Science Foundation of China (81900846) and Tianjin Key Medical Discipline (Specialty) Construction Project (TJYXZDXK-037A).

Authors' contributions

Methodology, YND, HS, ZHZ, YTL and HL; Conceptualization, XTC, HS; Validation and formal analysis, YND, CZ, HX and JWW; Writing—original draft preparation: YND; Writing—review and editing, XMZ; Supervision, XMZ; Funding acquisition, XTC. All authors have read and agreed to the published version of the manuscript.

Acknowledgements

Not applicable.

Authors' information

[1] Tianjin Key Laboratory of Retinal Functions and Diseases, Tianjin Branch of National Clinical Research Center for Ocular Disease, Eye Institute and School of Optometry, Tianjin Medical University Eye Hospital, Tianjin, China.

[2] Department of Ophthalmology and Visual Sciences, Kentucky Lions Eye Center, University of Louisville, School of Medicine, Louisville, KY, USA.

Reference

1. Selmi C. Diagnosis and classification of autoimmune uveitis. Autoimmun Rev. 2014;13(4-5):591-4.

2. Prete M, Dammacco R, Fatone MC, Racanelli V. Autoimmune uveitis: clinical, pathogenetic, and therapeutic features. Clin Exp Med. 2016;16(2):125-36.

3. Nozik RA. Periocular injection of steroids. Trans Am Acad Ophthalmol Otolaryngol. 1972;76(3):695-705.

4. Jea SY, Byon IS, Oum BS. Triamcinolone-induced intraocular pressure elevation: intravitreal injection for macular edema and posterior subtenon injection for uveitis. Korean J Ophthalmol. 2006;20(2):99-103.

5. Yoshikawa K, Kotake S, Ichiishi A, Sasamoto Y, Kosaka S, Matsuda H. Posterior sub-Tenon injections of repository corticosteroids in uveitis patients with cystoid macular edema. Jpn J Ophthalmol. 1995;39(1):71-6.

6. Oh JY, Lee RH. Mesenchymal stromal cells for the treatment of ocular autoimmune diseases. Prog Retin Eye Res. 2021;85:100967.

7. Tasso R, Ilengo C, Quarto R, Cancedda R, Caspi RR, Pennesi G. Mesenchymal stem cells induce functionally active T-regulatory lymphocytes in a paracrine fashion and ameliorate experimental autoimmune uveitis. Invest Ophthalmol Vis Sci. 2012;53(2):786-93.

8. Qin Y, Chan AM, Chang YL, Matynia A, Kouris NA, Kimbrel EA, et al. Human Embryonic Stem Cell-Derived Mesenchymal Stromal Cells Decrease the Development of Severe Experimental Autoimmune Uveitis in B10.RIII Mice. Ocul Immunol Inflamm.

2018;26(8):1228-36.

9. Yang C, Wu M, You M, Chen Y, Luo M, Chen Q. The therapeutic applications of mesenchymal stromal cells from human perinatal tissues in autoimmune diseases. Stem Cell Res Ther. 2021;12(1):103.

10. Eggenhofer E, Benseler V, Kroemer A, Popp FC, Geissler EK, Schlitt HJ, et al. Mesenchymal stem cells are short-lived and do not migrate beyond the lungs after intravenous infusion. Front Immunol. 2012;3:297.

11. Toma C, Pittenger MF, Cahill KS, Byrne BJ, Kessler PD. Human mesenchymal stem cells differentiate to a cardiomyocyte phenotype in the adult murine heart. Circulation. 2002;105(1):93-8.

12. Dlouhy BJ, Awe O, Rao RC, Kirby PA, Hitchon PW. Autograft-derived spinal cord mass following olfactory mucosal cell transplantation in a spinal cord injury patient: Case report. J Neurosurg Spine. 2014;21(4):618-22.

13. Vulliet PR, Greeley M, Halloran SM, MacDonald KA, Kittleson MD. Intra-coronary arterial injection of mesenchymal stromal cells and microinfarction in dogs. Lancet. 2004;363(9411):783-4.

14. Zhou Y, Yamamoto Y, Xiao Z, Ochiya T. The Immunomodulatory Functions of Mesenchymal Stromal/Stem Cells Mediated via Paracrine Activity. J Clin Med. 2019;8(7).

15. Zhang B, Yin Y, Lai RC, Tan SS, Choo AB, Lim SK. Mesenchymal stem cells secrete immunologically active exosomes. Stem Cells Dev. 2014;23(11):1233-44.

16. Gnecchi M, Danieli P, Malpasso G, Ciuffreda MC. Paracrine Mechanisms of Mesenchymal Stem Cells in Tissue Repair. Methods Mol Biol. 2016;1416:123-46.

17. Chen X, Shao H, Zhi Y, Xiao Q, Su C, Dong L, et al. CD73 Pathway Contributes to the Immunosuppressive Ability of Mesenchymal Stem Cells in Intraocular Autoimmune Responses. Stem Cells Dev. 2016;25(4):337-46.

18. Alcedo KP, Bowser JL, Snider NT. The elegant complexity of mammalian ecto-5'-nucleotidase (CD73). Trends Cell Biol. 2021;31(10):829-42.

19. Yegutkin GG. Nucleotide- and nucleoside-converting ectoenzymes: Important modulators of purinergic signalling cascade. Biochim Biophys Acta. 2008;1783(5):673-94.

20. T LR, Sanchez-Abarca LI, Muntion S, Preciado S, Puig N, Lopez-Ruano G, et al. MSC surface markers (CD44, CD73, and CD90) can identify human MSC-derived extracellular vesicles by conventional flow cytometry. Cell Commun Signal. 2016;14:2.

21. Bai L, Shao H, Wang H, Zhang Z, Su C, Dong L, et al. Effects of Mesenchymal Stem Cell-Derived Exosomes on Experimental Autoimmune Uveitis. Sci Rep. 2017;7(1):4323.

22. Dominici M, Le Blanc K, Mueller I, Slaper-Cortenbach I, Marini F, Krause D, et al. Minimal criteria for defining multipotent mesenchymal stromal cells. The International Society for Cellular Therapy position statement. Cytotherapy. 2006;8(4):315-7.

23. Jian R, Yang M, Xu F. Lentiviral-mediated silencing of mast cell-expressed membrane protein 1 promotes angiogenesis of rats with cerebral ischemic stroke. J Cell Biochem. 2019;120(10):16786-97.

24. Livak KJ, Schmittgen TD. Analysis of relative gene expression data using real-time quantitative PCR and the 2(-Delta Delta C(T)) Method. Methods. 2001;25(4):402-8.

25. Witwer KW, Buzas EI, Bemis LT, Bora A, Lasser C, Lotvall J, et al. Standardization of sample collection, isolation and analysis methods in extracellular vesicle research. J Extracell

Vesicles. 2013;2.

26. Agarwal RK, Caspi RR. Rodent models of experimental autoimmune uveitis. Methods Mol Med. 2004;102:395-419.

27. Gadjanski I, Williams SK, Hein K, Sattler MB, Bahr M, Diem R. Correlation of optical coherence tomography with clinical and histopathological findings in experimental autoimmune uveoretinitis. Exp Eye Res. 2011;93(1):82-90.

28. Li Y, Ren X, Zhang Z, Duan Y, Li H, Chen S, et al. Effect of small extracellular vesicles derived from IL-10-overexpressing mesenchymal stem cells on experimental autoimmune uveitis. Stem Cell Res Ther. 2022;13(1):100.

29. Li Z, Liu F, He X, Yang X, Shan F, Feng J. Exosomes derived from mesenchymal stem cells attenuate inflammation and demyelination of the central nervous system in EAE rats by regulating the polarization of microglia. Int Immunopharmacol. 2019;67:268-80.

30. Mao F, Wu Y, Tang X, Kang J, Zhang B, Yan Y, et al. Exosomes Derived from Human Umbilical Cord Mesenchymal Stem Cells Relieve Inflammatory Bowel Disease in Mice. Biomed Res Int. 2017;2017:5356760.

31. Wang G, Yuan J, Cai X, Xu Z, Wang J, Ocansey DKW, et al. HucMSC-exosomes carrying miR-326 inhibit neddylation to relieve inflammatory bowel disease in mice. Clin Transl Med. 2020;10(2):e113.

32. Li Y, Altemus J, Lightner AL. Mesenchymal stem cells and acellular products attenuate murine induced colitis. Stem Cell Res Ther. 2020;11(1):515.

33. Shigemoto-Kuroda T, Oh JY, Kim DK, Jeong HJ, Park SY, Lee HJ, et al. MSC-derived Extracellular Vesicles Attenuate Immune Responses in Two Autoimmune Murine Models: Type

1 Diabetes and Uveoretinitis. Stem Cell Reports. 2017;8(5):1214-25.

34. Li H, Zhang Z, Li Y, Su L, Duan Y, Zhang H, et al. Therapeutic Effect of Rapamycin-Loaded Small Extracellular Vesicles Derived from Mesenchymal Stem Cells on Experimental Autoimmune Uveitis. Front Immunol. 2022;13:864956.

35. Hasko G, Linden J, Cronstein B, Pacher P. Adenosine receptors: therapeutic aspects for inflammatory and immune diseases. Nat Rev Drug Discov. 2008;7(9):759-70.

36. Naganuma M, Wiznerowicz EB, Lappas CM, Linden J, Worthington MT, Ernst PB. Cutting edge: Critical role for A2A adenosine receptors in the T cell-mediated regulation of colitis. J Immunol. 2006;177(5):2765-9.

37. Lappas CM, Rieger JM, Linden J. A2A adenosine receptor induction inhibits IFN-gamma production in murine CD4+ T cells. J Immunol. 2005;174(2):1073-80.

38. Sevigny CP, Li L, Awad AS, Huang L, McDuffie M, Linden J, et al. Activation of adenosine 2A receptors attenuates allograft rejection and alloantigen recognition. J Immunol. 2007;178(7):4240-9.

39. Erdmann AA, Gao ZG, Jung U, Foley J, Borenstein T, Jacobson KA, et al. Activation of Th1 and Tc1 cell adenosine A2A receptors directly inhibits IL-2 secretion in vitro and IL-2-driven expansion in vivo. Blood. 2005;105(12):4707-14.

40. Deaglio S, Dwyer KM, Gao W, Friedman D, Usheva A, Erat A, et al. Adenosine generation catalyzed by CD39 and CD73 expressed on regulatory T cells mediates immune suppression. J Exp Med. 2007;204(6):1257-65.

41. Ohta A, Kini R, Ohta A, Subramanian M, Madasu M, Sitkovsky M. The development and immunosuppressive functions of CD4(+) CD25(+) FoxP3(+) regulatory T cells are under

influence of the adenosine-A2A adenosine receptor pathway. Front Immunol. 2012;3:190.

42. Antonioli L, Pacher P, Vizi ES, Hasko G. CD39 and CD73 in immunity and inflammation. Trends Mol Med. 2013;19(6):355-67.

43. Yang J, Liao X, Yu J, Zhou P. Role of CD73 in Disease: Promising Prognostic Indicator and Therapeutic Target. Curr Med Chem. 2018;25(19):2260-71.

44. Ko MK, Shao H, Kaplan HJ, Sun D. CD73(+) Dendritic Cells in Cascading Th17 Responses of Experimental Autoimmune Uveitis-Induced Mice. Front Immunol. 2020;11:601272.

45. Amarnath S, Foley JE, Farthing DE, Gress RE, Laurence A, Eckhaus MA, et al. Bone marrow-derived mesenchymal stromal cells harness purinergenic signaling to tolerize human Th1 cells in vivo. Stem Cells. 2015;33(4):1200-12.

46. Huang F, Chen M, Chen W, Gu J, Yuan J, Xue Y, et al. Human Gingiva-Derived Mesenchymal Stem Cells Inhibit Xeno-Graft-versus-Host Disease via CD39-CD73-Adenosine and IDO Signals. Front Immunol. 2017;8:68.

47. Gao ZW, Wang HP, Lin F, Wang X, Long M, Zhang HZ, et al. CD73 promotes proliferation and migration of human cervical cancer cells independent of its enzyme activity. BMC Cancer. 2017;17(1):135.

48. Qiao Z, Li X, Kang N, Yang Y, Chen C, Wu T, et al. A Novel Specific Anti-CD73 Antibody Inhibits Triple-Negative Breast Cancer Cell Motility by Regulating Autophagy. Int J Mol Sci. 2019;20(5).

49. Qin H, Sun C, Kong D, Zhu Y, Shao B, Ren S, et al. CD73 mediates the therapeutic effects of endometrial regenerative cells in concanavalin A-induced hepatitis by regulating CD4(+) T

cells. Stem Cell Res Ther. 2023;14(1):277.

50. Lee JJ, Jeong HJ, Kim MK, Wee WR, Lee WW, Kim SU, et al. CD39-mediated effect of human bone marrow-derived mesenchymal stem cells on the human Th17 cell function. Purinergic Signal. 2014;10(2):357-65.

51. Hernandez-Mir G, McGeachy MJ. CD73 is expressed by inflammatory Th17 cells in experimental autoimmune encephalomyelitis but does not limit differentiation or pathogenesis. PLoS One. 2017;12(3):e0173655.

Supplementary Files

This is a list of supplementary files associated with this preprint. Click to download.

- AuthorChecklistFull.pdf
- figureS1.bmp
- FigureS2.bmp